Accepted Manuscript

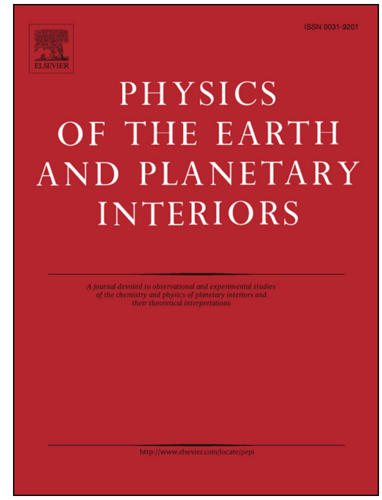

Dynamic triggering of earthquakes is promoted by crustal heterogeneities and bimaterial faults

Sebastian Langer, Yaron Finzi, Louise Marie Olsen-Kettle

PII: S0031-9201(14)00223-4
DOI: http://dx.doi.org/10.1016/j.pepi.2014.10.012
Reference: PEPI 5793

To appear in: *Physics of the Earth and Planetary Interiors*

Please cite this article as: Langer, S., Finzi, Y., Marie Olsen-Kettle, L., Dynamic triggering of earthquakes is promoted by crustal heterogeneities and bimaterial faults, *Physics of the Earth and Planetary Interiors* (2014), doi: http://dx.doi.org/10.1016/j.pepi.2014.10.012

Dynamic triggering of earthquakes is promoted by crustal heterogeneities and bimaterial faults

Sebastian Langer[a,*], Yaron Finzi[b], Louise Marie Olsen-Kettle[a]

[a] *Centre for Geoscience Computing, School of Earth Sciences, The University of Queensland, Brisbane, Australia.*
[b] *Dead Sea & Arava Science Centre, Mitzpe Ramon, Israel.*

Abstract

Remotely triggered earthquakes and aftershocks constitute a great challenge in assessing seismic risk. A growing body of observations indicates that significant earthquakes can be triggered by moderate to great earthquakes occurring at distances of up to thousands of kilometers. Currently we lack the knowledge to predict the location of triggered events. We present numerical simulations showing that dynamic interactions between material heterogeneities (e.g. compliant fault zones, sedimentary basins) and seismic waves focus and enhance stresses sufficiently to remotely trigger earthquakes. Numerical simulations indicate that even at great distances (>100km), the amplified transient dynamic stress near heterogeneities is equivalent to stress levels near the source rupture tip (<5km). Such stress levels are widely considered capable of nucleating an earthquake rupture on a pre-stressed fault. Analysis of stress patterns in dynamic rupture simulations which include a heterogeneous zone with a range of material and geometrical properties reveals various mechanisms of stress enhancement. We conclude that both stiff

*Corresponding author. Tel.: +49 351 321 66988.
Email address: s.langer@uq.edu.au (Sebastian Langer)
URL: http://geocomp.uq.edu.au (Sebastian Langer)

and weak heterogeneities may focus stress waves to form zones of enhanced stress, and that bimaterial interfaces distort under static and dynamic loading in a way that induces local stress concentrations. Our work provides insights for understanding non-uniform distribution of remotely triggered seismicity and recurrence of such events along complex fault-systems and near magmatic intrusions and geothermal zones.

Keywords: remotely triggered seismicity, dynamic rupture simulation, forecasting earthquake interaction, stress shadow, bimaterial interface, fault-system stability, seismic wave amplification

---

1. Introduction

Earthquake triggering is the process by which stress changes associated with an earthquake can induce or retard seismic activity in the surrounding region. Static stress changes are permanent and produce increased seismicity rates where stress increases (stress triggering), or decreased seismicity rates where stress decreases (stress shadowing). Calculations of static Coulomb stress transfer have proven to be a powerful tool in explaining near-field aftershock distributions (King et al., 1994; Stein et al., 1997; Harris and Simpson, 1998; Pondard et al., 2007; Sumy et al., 2014). Dynamic stress changes due to the passage of seismic waves cause transient dynamic stress oscillations and as such are positive everywhere at some point in time. The physical origin of dynamic triggering remains one of the least understood aspects of earthquake nucleation. We assess some of the mechanisms involved in dynamic triggering. The majority of previous studies have focused on near-field static stress changes that trigger aftershocks, and some studied dynamic stress patterns near fault tips (Finzi and Langer, 2012a,b; Lozos et al., 2012). However in this work we focus on dynamic triggering far away from the fault and aim to elucidate some of the path-dependent mechanisms occuring in RTS. While these mechanisms are also present in near field we focus on remote triggering far away from the earthquake source where the contributions from the static stress changes are small and the path-dependent dynamic effects are dominant. The current work reveals how certain fault-zone structures may dynamically amplify and focus seismic waves and induce nucleation of RTS. While a great amount of attention has focused on forecasting near-field aftershocks the topic of RTS remains a great challenge in seismic hazard analysis.

Remotely triggered seismicity (RTS) has been reported following numerous large earthquakes such as the 2002, M7.9 Denali and the 1992, M7.3 Landers earthquakes (Eberhart-Phillips et al., 2003; Steacy et al., 2005; Hill et al., 1993). RTS at extremely large distances (>1000 km) has been associated with passing S and surface waves (Gomberg and Davis, 1996; Kilb et al., 2000; Gomberg et al., 2003; Lei et al., 2011). In fact, RTS is often described as the result of extremely weak stress perturbations acting on critically stressed faults (van der Elst and Brodsky, 2010). We investigate another mechanism of importance in RTS, where low amplitude stress pertubations may be amplified sufficiently by certain tectonic structures or heterogeneities to induce nucleation along faults that are not necessarily critically stressed.

Dynamic stress waves also affect induced seismicity in the near-field as they do far from the source event. Examples include reported seismicity following moderate ($M<7$) earthquakes (Hough, 2005) and dynamically triggered complex multi-segment earthquake sequences (Finzi and Langer, 2012a; Hill and Prejean, 2007; Hough, 2005). In fact, dynamic stress waves and their interaction with various fault structures is often considered as an explanation for aftershock patterns that deviate from those of static stress patterns (Freed, 2005).

To date, the underlying mechanisms for remote triggering remain a matter of continuing debate (Brodsky and Prejean, 2005; Prejean and Hill, 2009; Lei et al., 2011; Gomberg, 2013). It is well established that directivity effects can cause enhanced RTS in the rupture direction (Gomberg, 2013). However directivity and other source related effects cannot always fully explain why in some cases faults close to the source remain inactive whereas for the same earthquake distant faults are triggered. Therefore additional information such as path-dependent effects and local stress amplifications are required in order to determine if a fault-zone is likely to experience RTS. Recently, stress amplification on remote faults was also shown to be associated with dynamic interactions between seismic waves and geological structures (Gomberg, 2013). In her paper, Gomberg (2013) proposes that certain fault structures repeatedly experience RTS due to local dynamic interactions with passing seismic waves. In this paper we elucidate the mechanisms underpinning these interactions.

Many studies have shown how structural features such as low-velocity fault zones (Fohrmann et al., 2004) or sedimentary basins (Gomberg et al., 2004; Hartzell et al., 2010) can cause trapped waves and seismic wave amplification. Stress-enhancing interactions were also described in studies of wave reflection off the Moho or the Earth's core (Lin, 2010; Hough, 2007) and dynamic stress concentration along bimaterial interfaces (Stoneley, 1924; Burridge, 1973; Finzi and Langer, 2012a; Lei et al., 2011). While the phenomena of "seismic waves focusing", excitation of bimaterial interfaces and large scale wave reflections have long been studied in various geophysical contexts, only a few recent studies account for such processes in the context of remotely triggered seismicity (Lin, 2010; Lei et al., 2011; Gomberg, 2013).

We extend these studies by showing numerically how significant stress concentrations due to material heterogeneities far from a source earthquake may induce remotely triggered seismicity. We show how even smaller magnitude earthquakes can trigger far-field seismicity by considering the effect of crustal heterogeneities such as fault zones, basins and igneous bodies. While other studies (Fohrmann et al., 2004; Gomberg, 2013) have solely focused on the interactions between seismic waves and low-velocity zones, we demonstrate how dynamic interactions between the seismic waves and both compliant and stiff geological structures may induce remotely triggered seismicity in and around these structures.

2. Methods

2.1. Numerical simulations of dynamic stress transfer in a heterogeneous crust

In order to simulate remotely triggered seismicity we set up a Finite Element model domain where we solve the wave equation for dynamic rupture at a fault. Excitation of distant faults and bimaterial interfaces is studied by calculating Coulomb Failure Stress (CFS) throughout the model domain and by noting potentially significant occurrences of anomalously low and high values. Two principal triggering criteria are used to measure the likelihood of RTS. One is the threshold of peak transient CFS of the radiating seismic waves (Hill et al., 1993; Gomberg et al., 1997). A second criterion calculates the magnitude of the cumulative energy exerted at the fault (Brodsky et al., 2000). In the discussion we compare these two measures and show they give slightly different estimations of the likelihood of RTS.

We show that path effects are as important as source effects for RTS by examining the dynamic stress-enhancing interactions between seismic waves and heterogeneities embedded in the model domain. While most natural heterogeneities represent weakened zones such as damaged fault-zones and sedimentary basins, we also examine stress-enhancing interactions in the presence of a stiff zone (e.g. Vauchez et al. (1998) and Tommasi et al. (1995)). This enables a better understanding of the various stress-enhancing mechanisms.

We simulate tectonic loading and dynamic rupture using the same method as our previous study of multi-segment dynamic stress patterns (Finzi and

Langer, 2012a). We use the 2D finite element code esys.escript (Gross et al., 2007). The fault (see Figure 1) is embedded in a homogeneous medium with rigidity $G_0 = 30\,\mathrm{GPa}$, first Lame parameter $\lambda = 30\,\mathrm{GPa}$, density $\rho = 2700\,\mathrm{kg/m^3}$ and shear wave velocity $v_S = 3333\,\mathrm{m/s}$. The model domain is loaded with a stress tensor such that the unruptured source fault is optimally aligned with respect to the Coulomb Failure stress under the condition of a static coefficient of friction $\mu_s = 0.6$ (for more modelling constraints see Supplementary material).

The simulated earthquakes along the source fault are 60 km long with M_w7, an average slip of approximately 5 m and a maximum slip of 9 m at hypocentral depth (values chosen to be consistent with geologic observations; Wells and Coppersmith (1994)). Furthermore, the prescribed fault friction parameters ensure that simulated earthquakes exhibit sub-shear pulse-like ruptures.

A material heterogeneity in the form of a compliant/stiff zone of 8 km by 16 km is located at one fault length or 60 km East of the source fault (model A). Simulation results for two fault lengths separation between model and heterogeneity zone (model B) can be found in the Supplementary material section. The compliant material zone has a rigidity $G_A = 0.7\,\mathrm{G_0}$. As the first Lame parameter and density are kept unchanged, the shear wave speed in the heterogeneity is $v_A = \sqrt{0.7}\,\mathrm{v_S}$. The material properties of the stiff zone are $G_A = 1.3\,\mathrm{G_0}$ and $v_A = \sqrt{1.3}\,\mathrm{v_S}$. While a material contrast of 30% is large in terms of typical lithology variations in the crust, it represents various tectonic

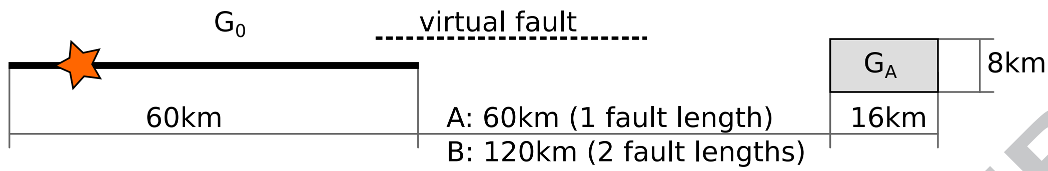

Figure 1: Model configuration for simulating dynamic stress to explore the occurrence of remotely triggered seismicity at the vicinity of material heterogeneities. The distance between the source earthquake and the heterogeneity is sufficient to assure that static stress changes induced by the earthquake are insignificant at the heterogeneity. The distance was either one fault length (model setup A) or two fault lengths (model setup B). The model has a background rigidity G_0 and the heterogeneity has a rigidity G_A. The virtual fault is used to calculate a normalized stress level.

settings in which soft sediments accumulate in a basin or accretionary prisms bounded by stiffer material (Gomberg (2013); Shani-Kadmiel et al. (2012, 2014); Hartzell et al. (2010) and DESERT group studies, e.g. Weber et al. (2009)) and across large faults such as the San Andreas (Brietzke and Ben-Zion (2006) and references therein). Figure 1 shows the configuration of our simulations, and other configurations used to test specific hypotheses are explained further in the discussion (see also Supplementary material for more details). Rupture is initiated at the star location in Figure 1 and after a short bilateral propagation phase, it proceeds unilaterally East towards the heterogeneous zone.

2.2. Analysis: peak transient CFS as a fault stability criterion

We conduct multiple dynamic rupture simulations assigning different elastic properties and geometrical characteristics to the material heterogeneity. To determine whether a rupture could nucleate on a remote fault in our

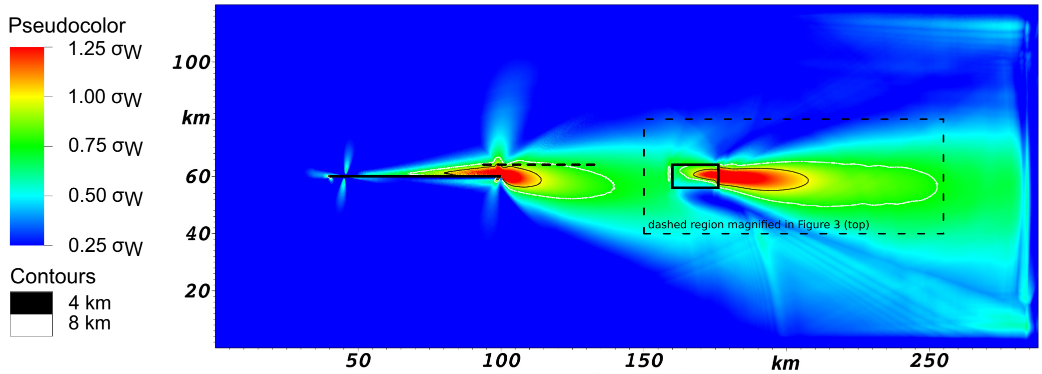

Figure 2: The normalised optimally oriented peak transient CFS is calculated such that the highest optimally aligned transient stress that occurs at the virtual fault (dashed line near primary fault) is set to $\sigma_W = 1$. All values above one suggest that triggering is likely to occur according to the "Wesnousky 4 km-rule".

model domain we calculate the peak transient Coulomb failure stress (peak transient CFS) on optimally oriented faults throughout the model domain. As in Finzi and Langer (2012a) we normalize the peak transient CFS values using its maximal value along a virtual fault parallel to the source fault at a distance of 4 km and with an overlap of 6 km (Figure 2). Normalizing by the stress level at a distance of 4 km, we adhere to a common assumption pertaining that ruptures are likely to jump step-overs as wide as 4 km but not wider (Wesnousky, 2006; Harris and Day, 1993). From this procedure it follows that normalised peak transient CFS values larger than 1 indicate that dynamic stresses may be sufficient to induce remotely triggered seismicity (on pre-stressed faults of suitable orientation).

3. Results

We describe the dynamic stress enhancement patterns in this section and in section 4 we discuss different possible mechanisms for the observed dynamic stress enhancement. Certain stress enhancement features in our results are analogous to those previously observed in simulations of dynamic stress patterns in fault step-over zones (Finzi and Langer, 2012a,b). For example, during the far-field loading of the model domain, (static) stress concentrations occur along the edges of the simulated material heterogeneity in the same way that was reported in simulations of segmented fault systems with weak step-over zones (Finzi and Langer, 2012b, Figure 4b). We therefore focus here on dynamic stress enhancement at large distances and refer the reader to our previous work for details on static stress concentrations at material heterogeneities.

3.1. Stress concentration along bimaterial interfaces and within the material heterogeneity

Simulations with compliant zones at large distances from the source earthquake exhibit significant stress concentrations along the leading (Western) and tailing (Eastern) bimaterial edges of such zones and within the weak zone (Figure 3). The normalised peak transient CFS pattern near the leading edge (marked X) exhibits elongated areas with increased stress. This can also be seen, albeit with lower stress magnitudes, West of the tailing edge interface (marked Y in Figure 3) and in simulations with a stiff heterogeneity

(Figure 4). Along the Northern edge of the heterogeneity there is an area (marked Z) with elevated peak transient CFS values. The area marked Z is located in the vicinity of a region of bimaterial contrast that experiences non-uniform straining when stressed.

3.2. Stress focusing by material heterogeneities

A prominent feature in all our simulated stress patterns consists of a very large stress lobe with high peak transient CFS values stretching from the weak zone away from the source event (Figures 2 and 3).The enhanced stress lobe for a compliant zone is comparable in size to the rupture length, and it exhibits peak transient CFS values as large as those observed at 2-3 km from the termination point of the source rupture. This stress lobe appears to radiate from near the heterogeneity and disperse/subside as the waves propagate away from the heterogeneity. In simulations with a material heterogeneity comprised of a stiff zone ($G_A = 1.3\,\mathrm{G}_0$), equivalent enhanced peak transient CFS lobes are formed, however there are two lobes stretching from near the Eastern corners of the heterogeneity and not oriented in the direction of rupture but rather in SE and NE directions (Figure 4) with the lobe in SE direction being stronger.

The difference in the strength of the lobes originates in a non-zero background stress for the CFS calculation and the different directions of the seismic waves. The Coulomb failure stress is calculated including the static portion for the normal and shear stress. The normal stress component of

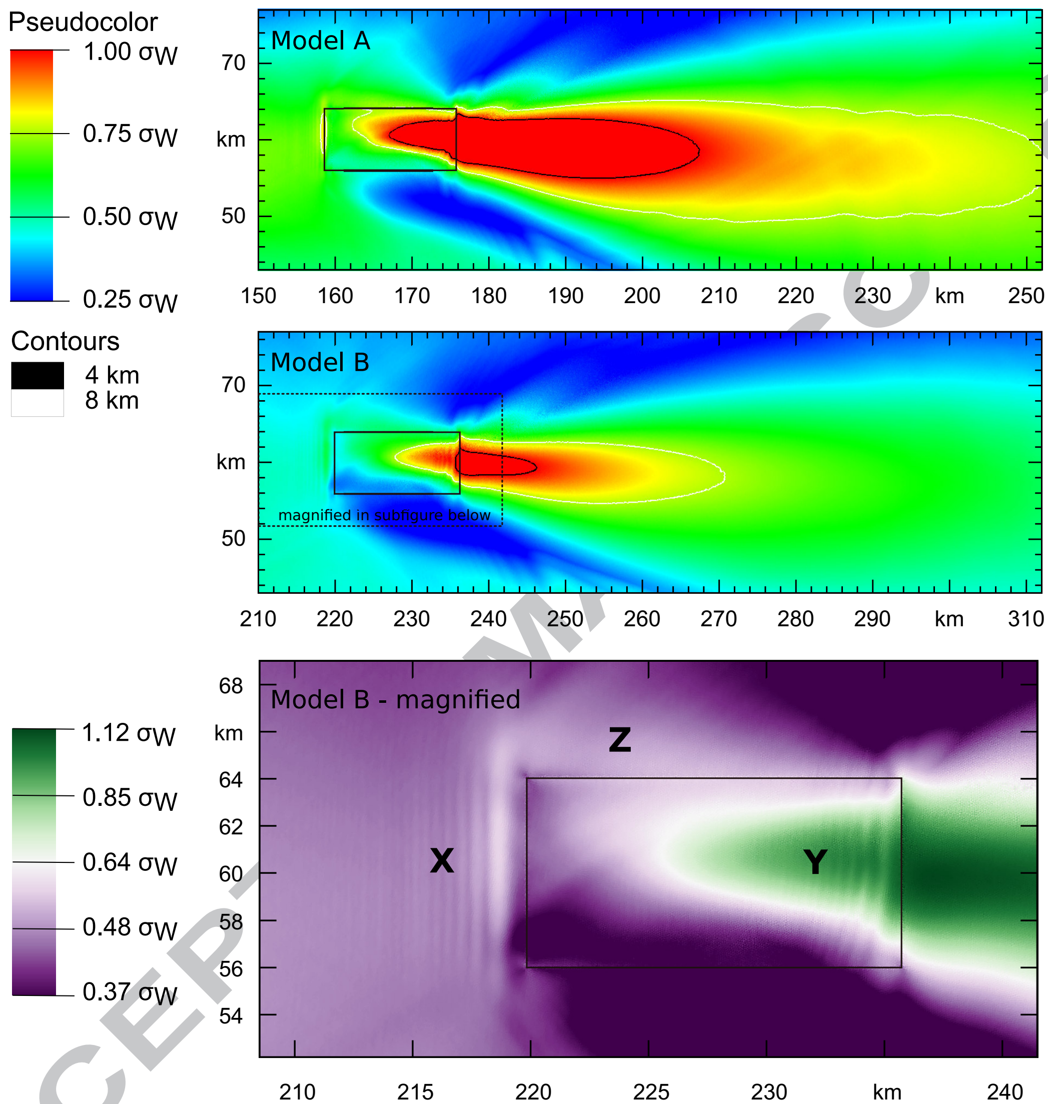

Figure 3: Close up view of stress patterns within the heterogeneity. Model A (top figure) shows the region around a compliant heterogeneity at 1 fault length away from the source fault and Model B (center figure) shows it at 2 fault lengths. The bottom figure shows an enlarged view of the center figure with a different color scale where Markers X and Y show patterns of equidistant elongated areas, Z shows elevated stress level outside the heterogeneity.

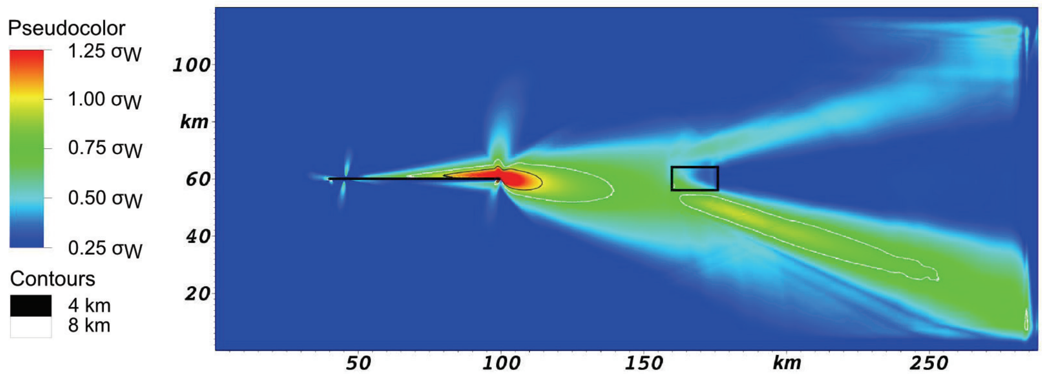

Figure 4: Enhanced stress beyond a stiff material heterogeneity. Simulation results exhibiting large lobes of enhanced peak transient CFS induced by stress wave focusing as they pass through the heterogeneity (see discussion and Figure 5). Stress waves seem to be diffracted / diverted to the SE direction forming a stress shadow East of the heterogeneity and enhanced peak transient CFS SE (and NE) of it.

the dynamic wave has an amplitude with opposite signs for waves travelling North and South. For further information see Supplementary material and Langer et al. (2010) for quasi-static tectonic loading.

4. Discussion

In interpreting our simulations we separate the stress-enhancing effects into two different groups. In the first subsection we explain effects that occur close to the heterogeneity due to strain contrasts and wave amplitude properties. In the second subsection we focus on effects that occur due to seismic ray path properties that change due to the heterogeneity.

4.1. Excitation of material interfaces

A wide range of studies have shown the various effects that bimaterial interfaces have on rupture processes and seismic wave propagation. Such studies include descriptions of strain patterns across bimaterial interfaces (Weertman, 1980; Cochard and Rice, 2000), and of unique surface waves that develop along such interfaces (Stoneley, 1924). The effect of bimaterial interfaces on rupture jumps over weak step-over zones separating fault segments was recently described in Finzi and Langer (2012b). Similarly, our current simulations show that dynamically propagating seismic waves induce stress enhancements along the bimaterial edges (Figures 2, 3, 4). Several mechanisms are plausible to explain the localized stress concentrations along the interfaces. These mechanisms include dynamic distortion due to the strain contrast across the interfaces and surface (Stoneley) waves along the locked interface. The higher CFS in area Z in Figure 3 is most likely caused by waves travelling along the bimaterial interface. A wave front extending perpendicular to an interface between different rigidities introduces a sharp gradient in the strain field and locally amplified stress. These mechanisms are not mutually exclusive and we cannot determine the relative contributions of each single mechanism.

4.2. Ray path processes (reflection, refraction, scattering, constructive/destructive interference and amplification/reduction of seismic waves at material heterogeneities)

The large stress lobes beyond the material heterogeneity show characteristics of focusing such as expected when waves travel through materials of different elastic properties. To verify that the observed stress concentrations are due to optical-like focusing we demonstrate this effect using a simplified model. We calculate ray paths that mimic seismic wave propagation from the source event (simplifying the source and representing it as a point source at the rupture termination point). Figure 5 shows the predicted wave propagation paths for seismic waves traveling through a weak zone ($G_A = 0.7\,\mathrm{G}_0$, Figure 5a) and through a stiff zone ($G_A = 1.3\,\mathrm{G}_0$, Figure 5b). It is expected that regions with overlapping ray paths may lead to elevated CFS and regions with sparser rays may represent lowered CFS (i.e. stress shadows). Figure 5 can be directly compared with Figure 2 and 4 and shows qualitatively a similar effect due to compliance or stiffness of the material heterogeneity. This simple model effectively demonstrates that ray path processes are important in RTS and may affect the ability to trigger earthquakes and the spatial distribution of triggered seismicity (a topic of recent studies; e.g. Brodsky and van der Elst (2014); van der Elst and Brodsky (2010)).

The elongated "ripples" West of the interfaces (marked X and Y in Figure 3) may be caused by a superimposition of the shear waves with their reflections at the bimaterial interface. The high peak transient CFS within the heterogeneities could be due to reflections along the top/bottom interfaces and/or interaction between the side interfaces that results in enhancement in a similar way that trapped waves and guided waves may be enhanced.

The ray path, scattering and bimaterial effects shown here to be important for dynamic stress amplifications depend on the wave frequency, the propagagtion length through the hetereogeneity and the relative size of the heterogeneity compared to the wavelength. These factors determine whether elastic focusing/defocusing (multipathing) effects or scattering effects due to the heterogeneity will dominate. Since the finite element method provides a full solution to the elastic wave equation, all the above properties are included and the direct, diffracted, converted and guided waves are modelled. Propagation of seismic waves and dynamically triggered seismicity will be affected by both elastic and anelastic properties. Anelastic effects are increasingly important as the frequency of the wave increases, leading to stronger damping of higher frequency waves. Although anelastic attenuation is not explicitly included in our numerical model, higher frequency wave amplitudes are artificially attenuated faster than lower frequency waves due to numerical dispersion and dissipation errors present in the finite element method. In this sense there is some form of anelastic attenuation present in our numerical model in addition to the elastic effects we explicitly include: geometrical spreading, elastic focusing/defocusing, scattering and amplification/reduction of seismic waves due to velocity contrast. We show the relative importance of elastic focusing/defocusing (multipathing) effects by demonstrating a good correlation between simulated stress patterns (Figures 2 – 4) and the ray paths calculated without incorporating anelastic or scattering effects (Figure 5).

4.3. Comparing alternative criteria for dynamic triggering

To assess the contribution of stress wave focusing in promoting rupture nucleation and triggered seismicity of a sharp bimaterial interface we construct a set of simulations with a material heterogeneity that has no sharp bimaterial interfaces. The rigidity is increasing smoothly from G_0 to G_A towards the center of the heterogeneity. We compare the resulting stress patterns to those in our typical simulations (e.g. compare Figure 6 with Figure 3) and to stress patterns in homogeneous simulations (see Supplementary material). We observe that the far-field effects that could be explained with wave focussing are still observed. However the interface effect along the bimaterial interfaces are missing or more likely distributed over a larger area and thus weaker.

4.4. Comparing the two measures used to estimate the likelihood of RTS

The cumulative effect of seismic waves can be determined by calculating the integrated energy density (Brodsky and Prejean, 2005). We present this property here as several researchers (Hill et al., 1993; Brodsky et al., 2000) assume cumulative energy to be important in triggering an earthquake. In Figure 7 we calculate the cumulative squared velocity $E_c = \int \dot{u}^2 dt$ as a proxy

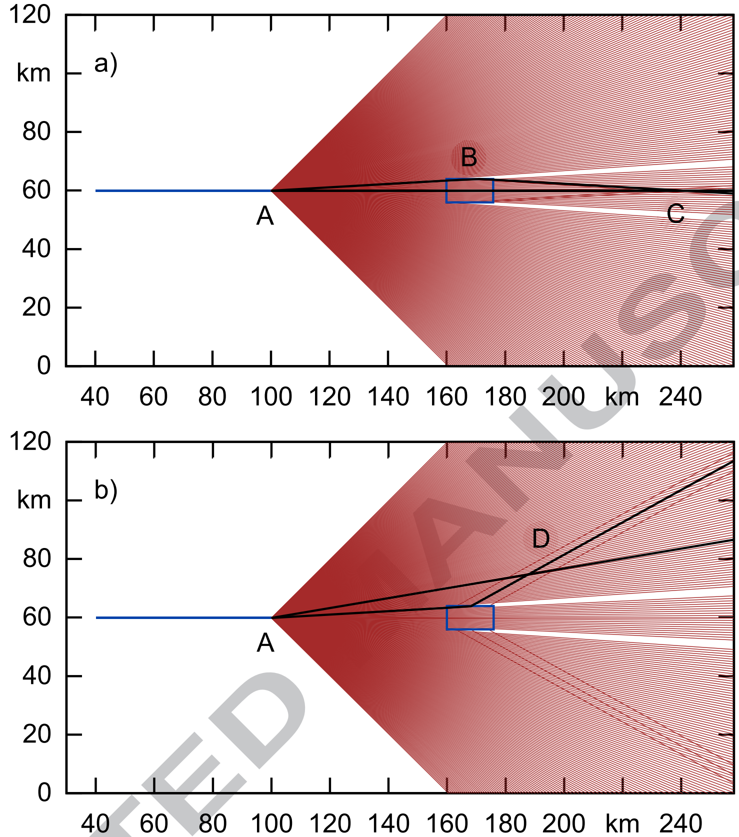

Figure 5: Calculated shear wave propagation paths using a simplified source model to compare with observed stress waves in FEM simulations with a) compliant (Figures 2, 3) and b) stiff (Figure 4) heterogeneities. Regions with overlapping ray paths are expected to have elevated CFS. As the reflected and non-reflected S-waves have similar ray path lengths there is only a slight delay. Wave crests may superimpose and increase peak transient CFS. In the stiff case (Figure b) this is partially due to the fact, that one path of overlapping waves has experienced an alteration in S-wave speed and the other has not. (A) shows the location of rupture arrest with a subset of emitted shear waves. (B) shows internal total reflection along the compliant zone interfaces. (C) shows the overlapping of ray path beyond the compliant zone and (D) shows the overlapping of ray paths past the stiff zone.

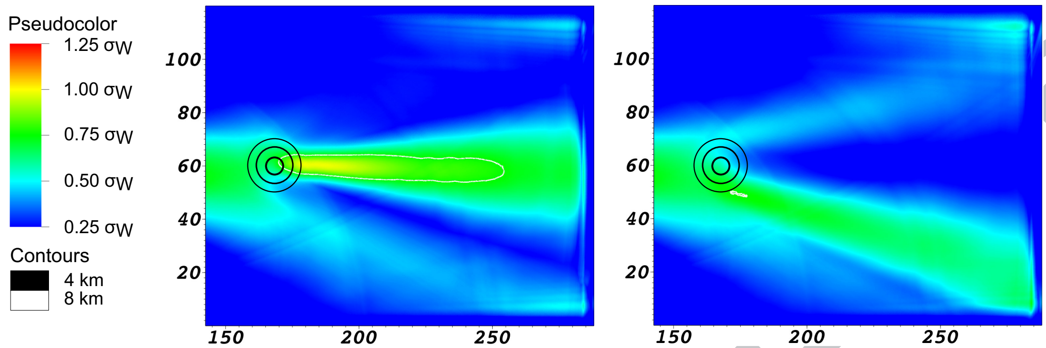

Figure 6: Comparing stress patterns in simulations with a circular heterogeneity with gradual transition between the materials, on the left with a compliant material anomaly and on the right with a stiff material anomaly.

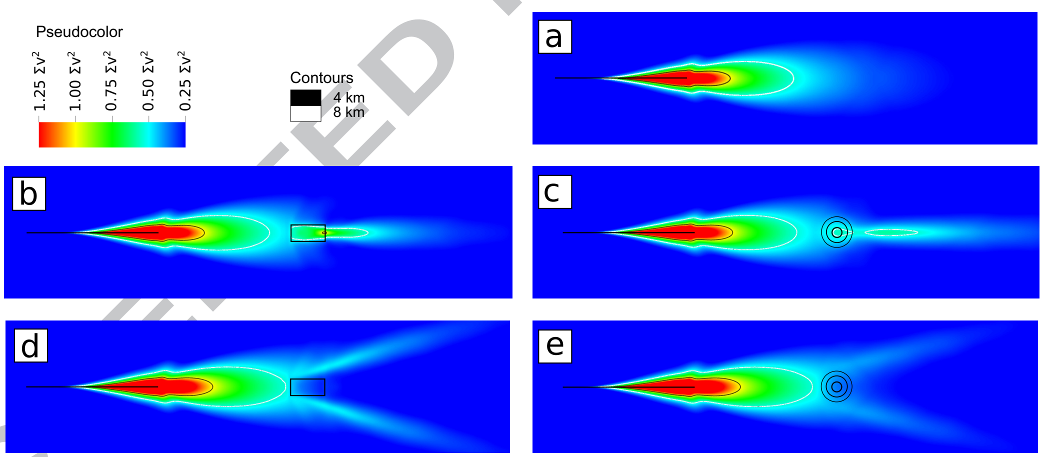

Figure 7: Overview showing normalized integrated squared velocity over the whole simulation time for a) no heterogeneity, b) a compliant rectangular bimaterial heterogeneity, c) a compliant circular smooth heterogeneity, d) a stiff rectangular bimaterial heterogeneity, e) a stiff circular smooth heterogeneity.

for integrated energy density. We normalise E_c to $E_{cn} = 1$ for the highest value of E_c at the virtual fault from Figure 1. From Figure 7 we can see that:

1. In contrast to the plot with peak transient CFS the integrated energy density is symmetric about the source fault. As mentioned in subsection 3.2 the asymmetry for peak transient CFS is due to non-zero background stress and the way CFS is calculated. The background particle velocity however is zero and therefore the amplitude of the velocity vector depends solely on the dynamic component of particle movement which results in a symmetric energy shape.
2. The focusing effect is significant even where the heterogeneity is not delimited by sharp bimaterial interfaces (see significant focusing in Figure 7c).
3. Only the superposition of the two effects (wave focusing and stress enhancement along interfaces) is sufficient to induce integrated energy density levels equivalent to those at $\approx 5\,\text{km}$ from the rupture tip (a level which suggest that RTS is plausible).
4. When comparing Figure 2 (top) and Figure 7b one can observe that the 'potentially unstable' region near the heterogeneity seems much smaller when considering the integrated energy index rather than the peak transient CFS as a triggering criteria. That is, the area confined by an 'energy level at 4 km' contour (Fig. 7b, black line) is much smaller than that outlined by the 'stress level at 4km' contour (Figure 2, black line). This shows that at least in our model the choice of an

indicator for seismic risk is important. Using the peak transient CFS as an indicator means a much larger region would have to be considered for seismic hazard assessment than if one used cumulative energy.

It has been shown in theoretical work on metamaterials (Farhat et al., 2012) and in experiments (Dubois et al., 2013), that complex geometry and material contrast may lead to local regions with low cumulative energy which is in agreement with Figure 7d. This supports the notion that natural stress focusing and stress shadows can be significant, and even could be as strong as in artificial seismic cloaking experiments (Brûlé et al., 2014).

At larger distances between source fault and the heterogeneity (>3-5 fault lengths) the focusing effect is expected to be minor compared to the effect of bimaterial interface excitation. This can be seen when comparing the two subfigures of Figure 3. The angle of reflecting waves along the top and bottom edges of the heterogeneity gets lower with distance to the source fault and thus less ray paths would be overlapping at similar location and time (see Figure 5). The size and geometry of the heterogeneity can have various effects on ray paths and stress enhancement. For example bent interfaces could have a large effect in dispersing or focusing stresses. The effect would depend on the direction of wave entry (like dispersing and converging lenses). Secondly the stress lobes in and outside the heterogeneity would change, as an elongated heterogeneity may behave like a fault zone that traps waves and enhances stress within and along the interfaces.

5. Conclusions and implications for Seismic Hazard Analysis

While numerous studies have indicated that dynamic stress may be large enough to trigger rupture at large distances from the source event, few provide explanations for the distribution and location of RTS and for the observations of recurring RTS. In such studies it is often assumed that prestress levels alone determine which faults are brought to failure by dynamic stress perturbations. This implies that until scientists are able to measure pre-stress levels on each fault, it would be impossible to identify faults and structures on which remotely triggered seismicity is more likely to occur. In the present study we show that geological structures can induce, enhance and focus stresses and achieve local CFS increase that is much higher than typically considered in studies of triggered seismicity. Such stress concentrations can trigger an earthquake on faults that would otherwise not be considered critically stressed. We propose a set of simple mechanisms that may be used to explain the occurrence (and recurrence) of remotely triggered seismicity, and to assess whether certain fault-zones are susceptible to RTS. In particular, our results show that geological structures (i.e. weak or stiff heterogeneities) can significantly influence stress enhancement and seismic wave focusing, and therefore can promote the occurrence of RTS. This conclusion is significantly supported by observations of geological structures that exhibited RTS following more than one source earthquake (e.g. geothermal zones exhibiting RTS after both the 1992 Landers and the 2002 Denali earthquakes; Hill et al. (1993); Prejean et al. (2004)). It is further supported by indication that seismic wave amplification, extended duration, and enhanced shaking along the Queen Charlotte sedimentary trough enabled the remote triggering of the 2013 M7.5 Craig Earthquake, British Columbia (Gomberg, 2013). Finally, our work asserts that geological structures such as accretionary prisms along subduction zones and sedimentary basins along transform plate boundaries may constitute zones of enhanced probability for dynamic triggering (as recently suggested by Gomberg (2013)). We therefore propose that detailed models of dynamic stress interactions should be used to identify fault zones that are likely to be triggered remotely by future earthquakes

6. Acknowledgment

We thank Ory Dor for his comments on an earlier version of the manuscript. We thank Vernon F. Cormier and an anonymous reviewer for their helpful review. Sebastian Langer thanks Louise Olsen-Kettle, the Centre for Geoscience Computing and the School of Earth Sciences at The University of Queensland for hosting his visit. Yaron Finzi acknowledges support by the Israel Ministry of Science, Technology and Space. Louise Olsen-Kettle is grateful for support from a University of Queensland Early Career Research Grant.

References

Brietzke, G. B., Ben-Zion, Y., nov 2006. Examining tendencies of in-plane rupture to migrate to material interfaces. Geophys. J. Int. 167, 807–819.

Brodsky, E. E., Karakostas, V., Kanamori, H., 2000. A new observation of dynamically triggered regional seismicity: Earthquakes in Greece following the August 1999 Izmit, Turkey earthquake. Geophysical Research Letters 27 (17), 2741–2744.

Brodsky, E. E., Prejean, S. G., 2005. New constraints on mechanisms of remotely triggered seismicity at Long Valley Caldera. Journal of Geophysical Research: Solid Earth (1978–2012) 110 (B4).

Brodsky, E. E., van der Elst, N. J., 2014. The Uses of Dynamic Earthquake Triggering. Annual Review of Earth and Planetary Sciences 42 (1), 317–339.
URL http://dx.doi.org/10.1146/annurev-earth-060313-054648

Brûlé, S., Javelaud, E. H., Enoch, S., Guenneau, S., 2014. Experiments on Seismic Metamaterials: Molding Surface Waves. Physical review letters 112 (13), 133901.

Burridge, R., 1973. Admissible Speeds for Plane-Strain Self-Similar Shear Cracks with Friction but Lacking Cohesion. Geophys. J. R. astr. Soc. 35 (4), 439–455.

Cochard, A., Rice, J. R., 2000. Fault rupture between dissimilar materials: Ill-posedness, regularization, and slip-pulse response. J. Geophys. Res. 105 (B11), 25,891–25,907.

Dubois, M., Farhat, M., Bossy, E., Enoch, S., Guenneau, S., Sebbah, P., 2013. Flat lens for pulse focusing of elastic waves in thin plates. Applied Physics Letters 103 (7).
URL http://scitation.aip.org/content/aip/journal/apl/103/7/10.1063/1.4818716

Eberhart-Phillips, D., Haeussler, P. J., Freymueller, J. T., Frankel, A. D., Rubin, C. M., Craw, P., Ratchkovski, N. A., Anderson, G., Carver, G. A., Crone, A. J., Dawson, T. E., Fletcher, H., Hansen, R., Harp, E. L., Harris, R. A., Hill, D. P., Hreinsdóttir, S., Jibson, R. W., Jones, L. M., Kayen, R., Keefer, D. K., Larsen, C. F., Moran, S. C., Personius, S. F., Plafker, G., Sherrod, B., Sieh, K., Sitar, N., Wallace, W. K., 2003. The 2002 Denali Fault Earthquake, Alaska: A Large Magnitude, Slip-Partitioned Event. Science 300 (5622), 1113–1118.
URL http://www.sciencemag.org/content/300/5622/1113.abstract

Farhat, M., Guenneau, S., Enoch, S., Jan 2012. Broadband cloaking of bending waves via homogenization of multiply perforated radially symmetric and isotropic thin elastic plates. Phys. Rev. B 85 (2), 020301.
URL http://link.aps.org/doi/10.1103/PhysRevB.85.020301

Finzi, Y., Langer, S., 2012a. Damage in Step-overs May Enable Large Cascading Earthquakes. Geophys. Res. Lett. 39, L16303.

Finzi, Y., Langer, S., 2012b. Predicting rupture arrests, rupture jumps and cascading earthquakes. J. Geophys. Res. 117 (B12), B12303.
URL http://dx.doi.org/10.1029/2012JB009544

Fohrmann, M., Igel, H., Jahnke, G., Ben-Zion, Y., 2004. Guided waves from sources outside faults: an indication for shallow fault zone structure? pure and applied geophysics 161 (11-12), 2125–2137.

Freed, A. M., 2005. Earthquake Triggering by Static, Dynamic, and Post-seismic Stress Transfer. Annual Review of Earth and Planetary Sciences 33 (1), 335.

Gomberg, J., 2013. Permanently enhanced dynamic triggering probabilities as evidenced by two M≥7.5 earthquakes. Geophysical Research Letters 40 (18), 4828–4833.

Gomberg, J., Blanpied, M. L., Beeler, N. M., 1997. Transient triggering of near and distant earthquakes. Bulletin of the Seismological Society of America 87 (2), 294–309.

Gomberg, J., Bodin, P., Larson, K., Dragert, H., feb 2004. Earthquake nucleation by transient deformations caused by the M = 7.9 Denali, Alaska, earthquake. Nature 427, 621–624.

Gomberg, J., Bodin, P., Reasenberg, P. A., 2003. Observing earthquakes triggered in the near field by dynamic deformations. Bulletin of the Seismological Society of America 93 (1), 118–138.

Gomberg, J., Davis, S., 1996. Stress/strain changes and triggered seismicity at The Geysers, California. Journal of Geophysical Research: Solid Earth (1978–2012) 101 (B1), 733–749.

Gross, L., Bourgouin, L., Hale, A. J., Muhlhaus, H. B., Aug. 2007. Interface Modeling in Incompressible Media using Level Sets in Escript. Physics of the Earth and Planetary Interiors 163, 23–34.

Harris, R. A., Day, S. M., 1993. Dynamics of Fault Interaction: Parallel Strike-Slip Faults. J. Geophys. Res. 98 (B3), 4461–4472.

Harris, R. A., Simpson, R. W., 1998. Suppression of large earthquakes by stress shadows: A comparison of Coulomb and rate-and-state failure. J. Geophys. Res. 103 (B10), 24439–24451.

Hartzell, S., Ramirez-Guzman, L., Carver, D., Liu, P., 2010. Short baseline variations in site response and wave-propagation effects and their structural causes: Four examples in and around the Santa Clara Valley, California. Bulletin of the Seismological Society of America 100 (5A), 2264–2286.

Hill, D. P., Prejean, S. G., 2007. Dynamic triggering. Treatise on Geophysics 4, 257–292.

Hill, D. P., Reasenberg, P. A., Michael, A., Arabaz, W. J., Beroza, G., Brumbaugh, D., Brune, J. N., Castro, R., Davis, S., Depolo, D., Ellsworth, W. L., Gomberg, J., Harmsen, S., House, L., Jackson, S. M., Johnston, M. J., Jones, L., Keller, R., Malone, S., Munguia, L., Nava, S., Pechmann, J. C., Sanford, A., Simpson, R. W., Smith, R. B., Stark, M., Stickney, M., Vidal, A., Walter, S., Wong, V., Zollweg, J., 1993. Seismicity Remotely

Triggered by the Magnitude 7.3 Landers, California, Earthquake. Science 260 (5114), 1617–1623.

Hough, S. E., 2005. Remotely triggered earthquakes following moderate mainshocks (or, why California is not falling into the ocean). Seismological Research Letters 76 (1), 58–66.

Hough, S. E., 2007. Remotely triggered earthquakes following moderate main shocks. SPECIAL PAPERS-GEOLOGICAL SOCIETY OF AMERICA 425, 73.

Kilb, D., Gomberg, J., Bodin, P., 2000. Earthquake triggering by dynamic stresses. Nature 408, 570–574.

King, G. C. P., Stein, R. S., Lin, J., 1994. Static stress changes and the triggering of earthquakes. Bull. Seismol. Soc. Am. 84 (3), 935–953.
URL `http://www.bssaonline.org/cgi/content/abstract/84/3/935`

Langer, S., Olsen-Kettle, L. M., Weatherley, D. K., Gross, L., Mühlhaus, H.-B., 2010. Numerical studies of quasi-static tectonic loading and dynamic rupture of bi-material interfaces. Concurrency Computat. Pract. Exper. 22 (12), 1684 – 1702.
URL `http://dx.doi.org/10.1002/cpe.1540`

Lei, X., Xie, C., Fu, B., 2011. Remotely triggered seismicity in Yunnan, southwestern China, following the 2004 Mw9. 3 Sumatra earthquake. Journal of Geophysical Research: Solid Earth (1978-2012) 116 (B8).

Lin, C.-H., 2010. A Large Mw 6.0 Aftershock of the 2008 Mw 7.9 Wenchuan Earthquake Triggered by Shear Waves Reflected from the Earth's Core. Bulletin of the Seismological Society of America 100 (5B), 2858–2865. URL `http://www.bssaonline.org/content/100/5B/2858.abstract`

Lozos, J. C., Oglesby, D. D., Brune, J. N., Olsen, K. B., 2012. Small intermediate fault segments can either aid or hinder rupture propagation at stepovers. Geophysical Research Letters 39 (18).

Pondard, N., Armijo, R., King, G. C. P., Meyer, B., Flerit, F., 2007. Fault interactions in the Sea of Marmara pull-apart (North Anatolian Fault): earthquake clustering and propagating earthquake sequences. Geophys. J. Int. 171 (3), 1185–1197.

Prejean, S. G., Hill, D. P., 2009. Earthquakes, dynamic triggering of. In: Encyclopedia of Complexity and Systems Science. Springer, pp. 2600–2621.

Prejean, S. G., Hill, D. P., Brodsky, E. E., Hough, S. E., Johnston, M. J. S., Malone, S. D., Oppenheimer, D. H., Pitt, A. M., Richards-Dinger, K. B., 2004. Remotely triggered seismicity on the United States West Coast following the Mw 7.9 Denali fault earthquake. Bulletin of the Seismological Society of America 94 (6B), –348.

Shani-Kadmiel, S., Tsesarsky, M., Louie, J. N., Gvirtzman, Z., 2012. Simulation of Seismic-Wave Propagation through Geometrically Complex Basins: The Dead Sea Basin. Bull. Seismol. Soc. Am. 102 (4), 1729–1739.

Shani-Kadmiel, S., Tsesarsky, M., Louie, J. N., Gvirtzman, Z., 2014. Geometrical focusing as a mechanism for significant amplification of ground motion in sedimentary basins: analytical and numerical study. Bulletin of earthquake engineering 12 (2), 607–625.

Steacy, S., Gomberg, J., Cocco, M., 2005. Introduction to special section: Stress transfer, earthquake triggering, and time-dependent seismic hazard. Journal of Geophysical Research: Solid Earth (1978–2012) 110 (B5).

Stein, R. S., Barka, A. A., Dieterich, J. H., mar 1997. Progressive failure on the North Anatolian fault since 1939 by earthquake stress triggering. Geophys. J. Int. 128, 594–604.

Stoneley, R., 1924. Elastic Waves at the Surface of Separation of Two Solids. Proceedings of the Royal Society of London. Series A, Containing Papers of a Mathematical and Physical Character 106 (738), 416–428.
URL http://www.jstor.org/stable/94262

Sumy, D. F., Cochran, E. S., Keranen, K. M., Wei, M., Abers, G. A., 2014. Observations of static Coulomb stress triggering of the November 2011 M5. 7 Oklahoma earthquake sequence. Journal of Geophysical Research: Solid Earth 119 (3), 1904–1923.

Tommasi, A., Vauchez, A., Daudré, B., 1995. Initiation and propagation of shear zones in a heterogeneous continental lithosphere. Journal of Geophysical Research: Solid Earth (1978–2012) 100 (B11), 22083–22101.

van der Elst, N. J., Brodsky, E. E., 2010. Connecting near-field and far-field earthquake triggering to dynamic strain. Journal of Geophysical Research: Solid Earth (1978–2012) 115 (B7).

Vauchez, A., Tommasi, A., Barruol, G., 1998. Rheological heterogeneity, mechanical anisotropy and deformation of the continental lithosphere. Tectonophysics 296 (1), 61–86.

Weber, M., Abu-Ayyash, K., Abueladas, A., Agnon, A., Alasonati-Tašárová, Z., Al-Zubi, H., Babeyko, A., Bartov, Y., Bauer, K., Becken, M., Bedrosian, P. A., Ben-Avraham, Z., Bock, G., Bohnhoff, M., Bribach, J., Dulski, P., Ebbing, J., El-Kelani, R., Förster, A., Förster, H. J., Frieslander, U., Garfunkel, Z., Goetze, H. J., Haak, V., Haberland, C., Hassouneh, M., Helwig, S., Hofstetter, A., Hoffmann-Rothe, A., Jäckel, K. H., Janssen, C., Jaser, D., Kesten, D., Khatib, M., Kind, R., Koch, O., Koulakov, I., Laske, G., Maercklin, N., Masarweh, R., Masri, A., Matar, A., Mechie, J., Meqbel, N., Plessen, B., Möller, P., Mohsen, A., Oberhänsli, R., Oreshin, S., Petrunin, A., Qabbani, I., Rabba, I., Ritter, O., Romer, R. L., Rümpker, G., Rybakov, M., Ryberg, T., Saul, J., Scherbaum, F., Schmidt, S., Schulze, A., Sobolev, S. V., Stiller, M., Stromeyer, D., Tarawneh, K., Trela, C., Weckmann, U., Wetzel, U., Wylegalla, K., 2009. Anatomy of the Dead Sea Transform from lithospheric to microscopic scale. Reviews of Geophysics 47 (2).
URL http://dx.doi.org/10.1029/2008RG000264

Weertman, J., 1980. Unstable slippage across a fault that separates elastic media of different elastic constants. J. Geophys. Res. 85(B3), 1455–1461.

Wells, D. L., Coppersmith, K. J., 1994. New empirical relationships among magnitude, rupture length, rupture width, rupture area, and surface displacement. Bull. Seismol. Soc. Am. 84 (4), 974–1002.
URL http://www.bssaonline.org/content/84/4/974.abstract

Wesnousky, S. G., 2006. Predicting the endpoints of earthquake ruptures. Nature 444 (7117), 358–360.

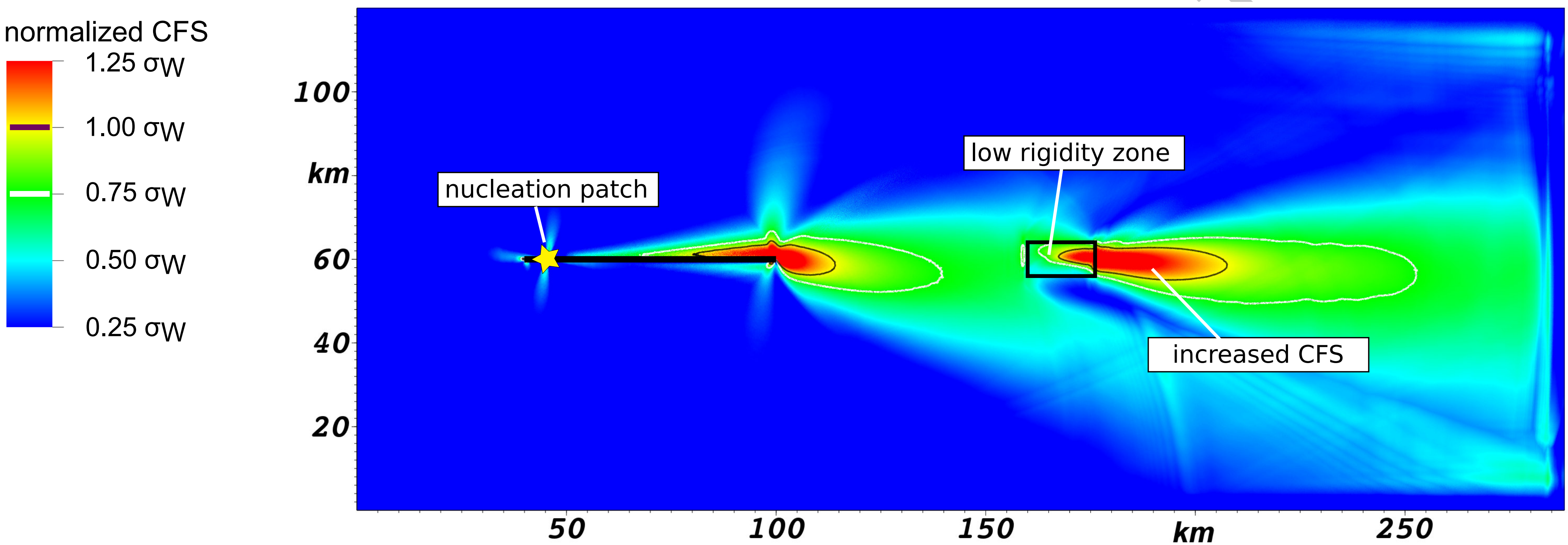

Pseudocolor plot of peak transient Coulomb failure stress (CFS): At $\sigma_W \geq 1$ remotely triggered rupture nucleation is likely.

We simulate dynamic fault rupture and stress interactions in a heterogeneous model.

Dynamic stress levels around and beyond heterogeneities are significantly amplified.

These increased stress levels are strong enough to trigger earthquakes.

Basins and weak fault-zones are prone to experience remotely triggered seismicity.